


Impact of Charge Regulation on Self-Assembly of Zwitterionic Nanoparticles

Jiaxing Yuan^{1,*}, Kyohei Takae,² and Hajime Tanaka^{1,2,†}¹*Research Center for Advanced Science and Technology, University of Tokyo,
4-6-1 Komaba, Meguro-ku, Tokyo 153-8904, Japan*²*Department of Fundamental Engineering, Institute of Industrial Science, University of Tokyo,
4-6-1 Komaba, Meguro-ku, Tokyo 153-8505, Japan* (Received 26 January 2022; accepted 18 March 2022; published 12 April 2022)

Zwitterionic modification of colloids with weak acids and bases represents a promising strategy in creating functional materials with tunable properties and modeling the self-organization of charged proteins. However, accurate incorporation of the dynamic dissociation or association of ionization groups known as charge regulation (CR) is often intractable in theoretical and computational investigations since charge redistribution and configuration need to be evolved self-consistently. Using hybrid Monte Carlo and molecular dynamics simulations, we demonstrate that a dilute suspension of overall charge-neutral zwitterionic Janus nanoparticles shows a conformational transition from an open assembly of string or bundle to compact cluster along with the variation in pH . The behavior under CR is qualitatively different from the commonly employed constant charge condition where the transition is absent. The CR-induced clustering is due to the inhomogeneous and fluctuating charges localized near the equatorial boundary of the Janus particle. These features are enhanced particularly at low salt concentration and high electrostatic coupling strength. Our results indicate the critical role of charge regulation in the spatial self-organization of zwitterionic nanoparticles.

DOI: [10.1103/PhysRevLett.128.158001](https://doi.org/10.1103/PhysRevLett.128.158001)

Janus particles, whose surfaces have two or more distinct physical or chemical properties, are attractive building blocks in the development of functional materials [1,2]. Their anisotropic nature has permitted diverse applications ranging from stimuli-responsive drug delivery carriers [3,4] to active swimmers with controlled movement [5,6]. Among the various types of Janus particles [7,8], zwitterionic particles with oppositely charged surface regions, also termed inverse patchy colloids, represent an important class [4,9–17]. For example, by coating the hemispheres with weak polymeric acid and base groups, pH -driven aggregation and disaggregation can be efficiently achieved [11,12]. The idea of reversible self-assembly has been utilized to construct a drug capsule with a controllable release of dual drug molecules [4]. The self-organization of zwitterionic particles is relevant not only to these advanced materials applications but also to understanding more complex biological phenomena, such as protein aggregation [18–20].

Given the prevalence of zwitterionic particles, extensive experimental [9–11,16,17], theoretical [21–24], and computational [10,16,25–27] investigations have been conducted on their self-assembly. The pioneering experimental investigation demonstrated that overall-neutral, zwitterionic Janus particles can form linear strings in solution [9], behaving as dipolar spheres [25,26]. Granick and co-workers also observed colloidal clusters in the condition that the particle diameter exceeds the Debye screening

length, providing valuable insights regarding the role of electrostatic screening [10]. Theoretical and computational approaches employing dipolar approximations or mean-field electrostatics have enabled the predictions of phase behavior upon system parameters, such as temperature [25,27], surface patch coverage [16,22,23,27], and volume fraction [25]. However, another important effect concerns the dynamic dissociation and association of surface ionization groups, which is commonly known as the charge regulation (CR) process [28–30]. Indeed, CR effects can mediate far richer complex electrostatic interactions between charged objects in various soft matter systems compared to the conventional constant charge (CC) condition [19,31–34]. It is also found that CR is responsible for the electrostatic phenomenon of like-charge attraction under a certain condition [18–20,35]. Moreover, recent particle-based simulations have revealed that CR effects can qualitatively change self-assembled structures in a binary suspension of colloidal particles with size asymmetry, stabilizing open aggregates, whereas the CC approximation results in the opposite trend [36]. From these prior investigations, it is expected that CR effects can influence the self-organization of zwitterionic particles, particularly when their size is a few times the Bjerrum length, such as nanoparticles.

Nevertheless, hitherto all theoretical and computational investigations of zwitterionic particles have widely adopted CC approximation [10,16,25–27]. Furthermore, a primary

focus has been put on micron-sized colloids, and the phase behavior of zwitterionic nanoparticles has been explored far less frequently. The understanding of CR effects in the self-assembly of zwitterionic particles is of significant importance not only from applications viewpoint [3,4,13,14] but also from fundamental physics on the many-body self-organization under a complex interplay among particle configuration, ion distribution, and ion association-dissociation.

In this Letter, we use an optimized simulation method that allows accurate and efficient modeling of thousands of individual ionizable groups [37]. With this method, we demonstrate that CR effects can qualitatively change the self-organization behavior in a prototypical suspension of charged Janus, overall-neutral zwitterionic nanoparticles, compared to the CC condition that ignores the inhomogeneity and fluctuation of individual surface charges. Our model system consists of N_c zwitterionic nanoparticles [see Fig. 1(a) for an illustration of $N_c = 2$ particles] whose two hemispheres are coated with n_A weak acid (n_A^0 groups at neutral state A^0 and n_A^- groups at dissociated state A^-) and n_B base groups (n_B^0 groups at neutral state B^0 and n_B^+ groups at dissociated state B^+). It also includes dissociated ions (protons H^+ and hydroxyl ions OH^-) and salt ions (monovalent cations S^+ and monovalent anions S^-) immersed in an implicit solvent characterized by a dielectric permittivity ϵ_{sol} . The acid and base groups undergo the following dissociation reactions: $A^0 \rightleftharpoons A^- + H^+$ and $B^0 \rightleftharpoons B^+ + OH^-$ with equilibrium reaction constants pK_a and pK_b , respectively. We also implement water autoprotolysis reactions $\emptyset \rightleftharpoons H^+ + OH^-$ with \emptyset the empty set due to implicit solvent and the grand-canonical ion exchange $\emptyset \rightleftharpoons S^+ + S^-$ with a reservoir at a given pH and chemical potential pI . These reactions are modeled using a newly developed simulation method [37].

Following the restricted primitive model [38,39], we represent ions as uniform spheres of diameter $\sigma = 2r = 0.72$ nm, a typical value of hydrated ions [40], and mass m . We study nanoparticles of diameter $D = 2R = 8\sigma \approx 6$ nm with $n_A = n_B = 186$ acid and base groups uniformly distributed on each hemisphere, following the electron distribution in the Thomson problem [41]. The excluded-volume effects are modeled through purely repulsive Weeks-Chandler-Andersen potential with an energy coupling $\epsilon = k_B T$. We consider overall-neutral zwitterionic Janus nanoparticles with $pK_a = pK_b = pK$. This setting enables us to isolate CR effects from the possible influences of net charge and hydrophobic (or van der Waals) attraction on the self-organization behavior. We consider the case of a long Bjerrum length $l_B = \beta q^2 / (4\pi\epsilon_{\text{sol}}) = 2\sigma$, where $\beta = 1/(k_B T)$, k_B is Boltzmann's constant, T is the absolute temperature, and q is the elementary charge. This choice enhances the electrostatic CR effects, but we will demonstrate that our observations hold at lower coupling ($l_B = \sigma$) as well. We adopt a choice of

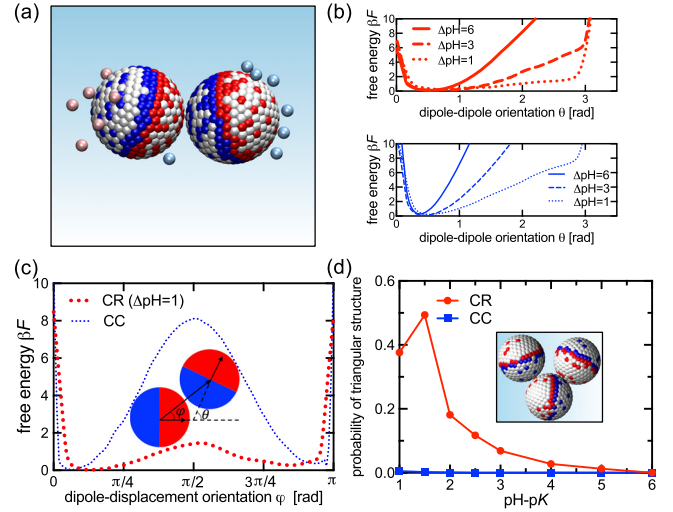


FIG. 1. Charge regulation effects on the effective interparticle interaction and the self-assembly for two and three zwitterionic nanoparticles. (a) Typical charge distribution of two zwitterionic nanoparticles in parallel alignment, showing negatively charged dissociated (blue) and neutral (white) acid groups, positively charged dissociated (red) and neutral (white) base groups, free cations (light red), and anions (light blue) at $\Delta pH = pH - pK = 6$ and $pI = 4$. (b) The free-energy profiles as a function of the relative dipole-dipole orientation θ [see the inset of (c) for the definition] at various ΔpH for CR nanoparticles (top) and CC nanoparticles (bottom) which can translate and rotate freely. Although the free-energy profiles qualitatively remain the same, CR allows a more substantial fluctuation in θ , indicating two nearby CR nanoparticles can more easily adjust their relative orientation. (c) The free-energy profiles as a function of the relative dipole-displacement orientation φ [see the inset of (c) for definition] at $\Delta pH = 1$ for CR nanoparticles (red dotted thick curve) and CC nanoparticles (blue dotted thin curve). We find that CR effects significantly reduce the free-energy barrier for the second nanoparticle rolling to the other side of the first nanoparticle. (d) The equilibrium probability of triangular configuration (see the inset) formed by three zwitterionic nanoparticles at various ΔpH . Here we adopt a criterion where two nanoparticles are considered bonded if their distance is smaller than 10σ . While linear string always remains dominant under the CC condition, CR boosts the probability of triangular configuration when $pH \sim pK$.

$pI = 4$, which ensures a dilute reservoir salt concentration $c_s = 10^{-4}$ M. This leads to a screening length $\lambda_D = (8\pi l_B c_s)^{-1/2} \approx 21$ nm for all pH values within $4 \leq pH \leq 10$, where only the difference $\Delta pH = pH - pK$ matters. We utilize a cubic simulation cell size $L = 100\sigma$ with a 3D periodic boundary condition. The long-range electrostatic interactions are calculated via the particle-particle mesh algorithm [42] with a relative force accuracy of 10^{-5} . Additional details and model limitations are presented in Supplemental Material [43].

To understand the role of CR effects, we first investigate how the CR regulates basic electrostatic interactions in systems consisting of $N_c = 2$ [Figs. 1(b) and 1(c)] and

$N_c = 3$ [Fig. 1(d)] nanoparticles. To this end, we perform free-energy calculations using the well-tempered metadynamics method [48,49]. Figure 1(b) shows the free-energy profiles βF for $N_c = 2$ as a function of the dipole-dipole orientation θ [see the inset of Fig. 1(c) for the definition of θ] for both CR [Fig. 1(b), top] and CC [Fig. 1(b), bottom] conditions. While the overall shape of βF is qualitatively the same, we can see that CR leads to a stronger θ fluctuation for small ΔpH . At $\Delta pH = 1$, fluctuation effects are the strongest. Nevertheless, the local minima of βF are not located at $\theta = 0$ due to the anisotropic charge distribution where surface charges are primarily induced near the equatorial Janus boundary region [cf. Fig. 1(a)]. Such anisotropic charge distribution is energetically favored because of the strong electrostatic attraction between surface disassociated acid and base groups. This phenomenon is more prominent at a smaller ΔpH . While the two nanoparticles could rotate to change the relative dipolar orientation under thermal fluctuation, a nanoparticle can also roll along the surface of the other particle toward its opposite side. Indeed, the free energy βF as a function of dipole-displacement orientation φ at $\Delta pH = 1$ [see the inset of Fig. 1(c) for the definition of φ and Fig. S1 in the Supplemental Material [43] for $\beta F(\varphi)$ at $\Delta pH = 6$] exhibits two local minima for both CR and CC conditions, as shown in Fig. 1(c). However, CR effects reduce the free-energy barrier height from $\beta F^* \approx 8k_B T$ under the CC approximation to $\beta F^* \approx 2k_B T$. The reduction in βF^* can also be explained by the anisotropic charge distribution that promotes the emergence of side-by-side arrangement (Fig. S2 in the Supplemental Material [43]), as often observed in CR simulations. The reduction in βF^* increases the probability of a nanoparticle rolling toward the opposite side. In addition, previous mean-field-level theories using a perturbation approach [19,50] have demonstrated that CR can introduce an attractive component into the intermolecular free energy; in particular, it becomes the dominant contribution when the mean charge is close to zero, which is exactly the case studied here. This theoretical prediction coincides with our simulations of $N_c = 3$ nanoparticles [Fig. 1(d)], where we indeed find that CR significantly boosts the equilibrium probability of compact triangular configuration [see the inset of Fig. 1(d)] at smaller ΔpH . On the other hand, a linear string instead of a compact triangle is always nearly 100% under the CC condition.

The above results suggest that CR effects may drastically influence the self-organization of many-particle systems. We examine this in two systems of $N_c = 10$ [corresponding to the volume fraction 2×10^{-3} , Figs. 2(a), 2(b), 2(e), and 2(f)] and $N_c = 30$ [corresponding to the volume fraction 6×10^{-3} , Figs. 2(c), 2(d), 2(g), and 2(h)] nanoparticles for both CR (Fig. 2, top) and CC (Fig. 2, bottom) conditions. We can see that CR effects indeed have drastic consequences on the self-organization behavior: open assembly

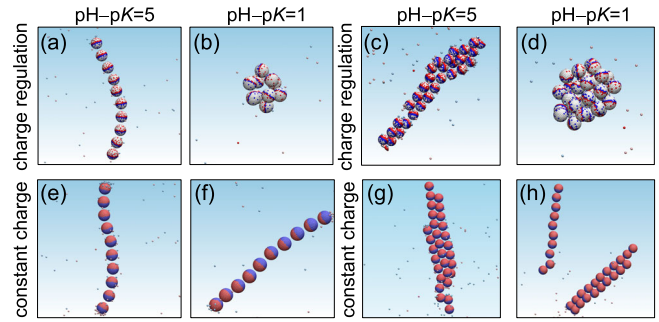


FIG. 2. Examples of the importance of charge regulation in electrostatically driven self-organization of zwitterionic nanoparticles. Typical equilibrium configuration of nanoparticle aggregates for systems containing $N_c = 10$ [$\Delta pH = pH - pK = 5$ in (a) and $\Delta pH = 1$ in (b)] and $N_c = 30$ [$\Delta pH = 5$ in (c) and $\Delta pH = 1$ in (d)] zwitterionic nanoparticles. To demonstrate the effects of CR, we also perform simulations (e)–(h) with CC nanoparticles, where each of the surface groups carries a constant charge that is determined from the average ionization of the CR particles. While the CC condition always gives rise to open assemblies (string at low N_c and bundle at large N_c), CR leads to a conformational transition to compact clusters at $pH \sim pK$. The color scheme used is the same as in Fig. 1.

of string or bundle (depending on particle number N_c) at large ΔpH and compact cluster at small ΔpH . This behavior is qualitatively different from the results in the CC approximation, where the conformational transition is absent along with the variation in pH (more precisely, the average surface charge). Arguably, compact clusters similar to Figs. 2(b) and 2(d) have been observed in zwitterionic colloids [10,16]. However, we emphasize that the clustering previously reported is typically induced either by attractive short-range interactions [16,51] or for a relatively large particle size compared to the electrostatic screening length [10]. This essentially differs from our system, where the clustering is achieved by electrostatic interactions alone without other interactions favoring clustering [51] and the size of zwitterionic nanoparticles is far smaller than electrostatic screening length. We also performed CC simulations where nanoparticles carry static equatorial charges and do not observe compact clusters. This implies that the anisotropic charge alone is insufficient to induce clustering in our systems, while the fluctuating nature of CR effects plays a critical role. Thus, we may say that our model system has the advantage of isolating CR effects, permitting an accurate assessment of their relevance in nanoparticle self-organization. To our knowledge, the CR effects on the self-assembly of zwitterionic particles discussed here have been overlooked.

One advantage of MD simulations is that their particle-level resolution allows a direct structural analysis of the cluster, given the experimental challenge of observing nanoscale building blocks in an aqueous medium. Here we characterize the structure by the radial density distribution $\rho(r)$, as shown in Fig. 3. The first main peak of $\rho(r)$

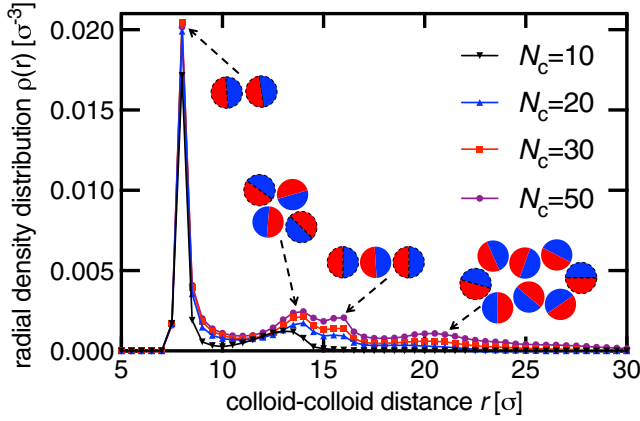


FIG. 3. Radial density distribution $\rho(r)$ of cluster aggregates formed by various nanoparticle numbers $N_c = 10$ – 50 at $\Delta pH = pH - pK = 1$. The peaks of $\rho(r)$ are labeled by the corresponding local particle arrangements within the cluster, where the distance r refers to that between nanoparticles with dashed lines.

appears at $r \approx D$ as expected, with a density value that is almost independent of $N_c \geq 30$. Notably, the emergence of the second peak at $r \approx \sqrt{3}D \simeq 14\sigma$ reflects the existence of a typical triangular arrangement, as depicted in Fig. 3, followed by the third peak at $r \approx 2D$ representing an alignment structure. For $N_c = 50$, the fourth peak also appears at $r \approx 2.6D$, which indicates a pentagonal arrangement, as shown in Fig. 3. The local coordination number z defined as the average number of particles within the first minimum of $\rho(r)$ from a chosen particle is estimated to be $z \approx 8.5$ for $N_c = 50$, which is much less than $z = 12$, an optimal packing for hard-sphere systems. Thus, the formed colloidal cluster can be seen as a loosely packed liquid droplet. This loose packing must be due to complex electrostatic interactions, consistent with the presence of pentagonal arrangements.

Finally, we present the full phase diagrams as a function of $\Delta pH = pH - pK$ and particle number N_c for both CR [Fig. 4(a)] and CC conditions [Fig. 4(b)]. While CR effects still permit the clustering for up to $N_c = 60$ nanoparticles, the transition point of ΔpH^* between open and compact structures shifts to a smaller value with increasing N_c [Fig. 4(a)]. We note that the conformational change along with ΔpH is accompanied by a monotonic variation in the ionization degree α , with a kink location of ΔpH^* that is consistent with the equilibrium conformation transition (see Fig. S3 in the Supplemental Material [43]). The variation in α , however, becomes smoother for large N_c , where the transition is absent. In contrast, a compact cluster is never observed under the CC approximations [Fig. 4(b)]. This difference highlights the essential roles of CR effects. Although there seems to be no limit to the size of clusters that can form from CR effects, the trend in Fig. 4(a) suggests that for larger N_c such a conformational transition

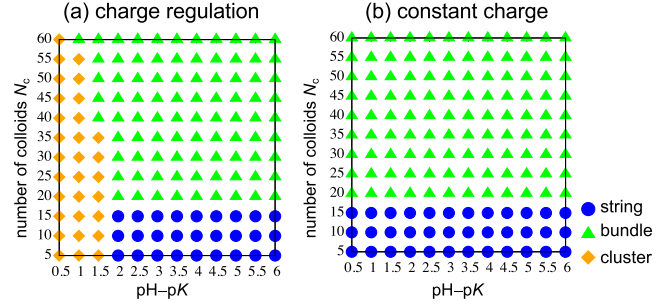


FIG. 4. General phase diagrams of overall-neutral charged Janus zwitterionic nanoparticles for both CR (a) and CC (b) conditions, covering a wide range of particle number N_c and $\Delta pH = pH - pK$. Consistent with Fig. 2, CR effects allow a conformational transition from string (blue circles) or bundle (light green triangles) to compact cluster (orange rhombus) along with the variation in ΔpH , whereas under the CC approximations the transition is absent. The clustering persists up to $N_c \sim 60$ nanoparticles, corresponding to a volume fraction of $\sim 1\%$, but a transition point ΔpH^* decreases with increasing N_c .

might not be observed. However, the finite-size effects have to be considered carefully. Analyzing the variance of the charge per particle $\sigma_Q^2 = \langle Q^2 \rangle - \langle Q \rangle^2$, we observe an eight-fold reduction in σ_Q^2 when increasing from $N_c = 5$ to $N_c = 50$ owing to less free space for each of the nanoparticles to move, indicating that CR effects are effectively suppressed in systems of larger N_c . Furthermore, we need to consider kinetic factors and metastability for larger N_c , where systems are likely trapped away from thermodynamic equilibrium; bundlelike aggregates are often observed experimentally when the volume fraction is high [52]. The observed colloidal clusters may also provide a (partial) explanation of protein aggregation near the isoelectric point [53] where anisotropic and fluctuating spatial charges should play crucial roles [18,54].

The observations presented here depend on the reservoir salt concentration c_s as well as the electrostatic coupling strength l_B . In Figs. 1–4, we adopt a dilute reservoir concentration $c_s = 10^{-4}$ M and an enhanced electrostatic coupling condition $l_B = 2\sigma$. We present the effect of the reservoir salt concentration on the clustering in Fig. S4 of the Supplemental Material [43] for $N_c = 10$ nanoparticles at $l_B = 2\sigma$ and $\Delta pH = 1$. It shows that increasing c_s , up to the physiological saline concentration leads to a gradual disassembly of the aggregated cluster due to the screened electrostatic interactions. We note that this predicted trend of nanoparticles differs from the behavior of micron-sized colloids, where screened electrostatic interactions result in the formation of clusters [10] but agrees with earlier simulations of nanoparticles [36]. The difference might arise from the absence of van der Waals attractive interaction [10]. For a shorter Bjerrum length l_B , the relative area of the cluster in the phase diagram becomes smaller (Fig. S5 in the Supplemental Material [43]), and the

transition eventually disappears under the CR condition for $N_c = 60$, suggesting that the CR effects become relatively weaker. These observations indicate that a lower reservoir salt concentration c_s and a longer Bjerrum length l_B (e.g., by mixing water with organic solvent) strengthens CR effects, increasing the stability of compact clusters. Comparing the electrostatic attraction between two particles ($6-7k_B T$ at $\Delta pH = 1$ in Fig. 1) with the typical van der Waals attraction between silica nanoparticles [$E_{vdW} = -(AR/12d) \sim -5k_B T$ for $R = 4\sigma$ and $d = \sigma$, where d is the interface separation and A is the Hamaker constant], the electrostatic CR effects can be comparable to the contribution from the van der Waals attraction for nanoparticle systems.

In conclusion, using an efficient and accurate method that permits coarse-grained molecular dynamics simulations of a wide range of solvated systems [37], we have elucidated the effects of charge regulation on the self-organization behavior in a prototypical suspension of overall-neutral zwitterionic Janus nanoparticles. We have revealed that along with the variation in pH , charge regulation effects result in a conformational transition from an open assembly of string or bundle to a compact cluster at $pH \sim pK$ for a dilute suspension, which is fundamentally different from the commonly employed constant charge approximation where the transition is absent. The clustering of nanoparticles arises due to inhomogeneous and fluctuating equatorial surface charged groups, with the effect particularly prominent under low reservoir salt concentration and high electrostatic coupling. Our work provides fundamental insights into the role of charge regulation, demonstrating a new avenue to control the self-organization of zwitterionic nanoparticles and facilitating the understanding of a broad range of biological self-assembly problems.

This work was supported by the Grants-in-Aid for Specially Promoted Research (JSPS KAKENHI Grant No. JP20H05619) and Innovative Areas of Softcrystal (JSPS KAKENHI Grant No. JP17H06375) from the Japan Society for the Promotion of Science (JSPS). J. Y. is grateful to Erik Luijten, Tine Curk, and Yanwei Wang for discussions on charge regulation and acknowledges the support from Shanghai Jiao Tong University via the scholarship for outstanding Ph.D. graduates.

*yuan@g.ecc.u-tokyo.ac.jp

†tanaka@iis.u-tokyo.ac.jp

- [1] Andreas Walther and Axel H. E. Müller, Janus particles: Synthesis, self-assembly, physical properties, and applications, *Chem. Rev.* **113**, 5194 (2013).
 [2] Jie Zhang, Bartosz A. Grzybowski, and Steve Granick, Janus particle synthesis, assembly, and application, *Langmuir* **33**, 6964 (2017).

- [3] Xiaomin Li, Lei Zhou, Yong Wei, Ahmed Mohamed El-Toni, Fan Zhang, and Dongyuan Zhao, Anisotropic growth-induced synthesis of dual-compartment Janus mesoporous silica nanoparticles for bimodal triggered drugs delivery, *J. Am. Chem. Soc.* **136**, 15086 (2014).
 [4] Eun Young Hwang, Min Jung Kang, Aamna Basheer, and Dong Woo Lim, Tunable decoupling of dual drug release of oppositely charged, stimuli-responsive anisotropic nanoparticles, *ACS Appl. Mater. Interfaces* **12**, 135 (2020).
 [5] Jing Yan, Ming Han, Jie Zhang, Cong Xu, Erik Luijten, and Steve Granick, Reconfiguring active particles by electrostatic imbalance, *Nat. Mater.* **15**, 1095 (2016).
 [6] Jie Zhang, Erik Luijten, Bartosz A. Grzybowski, and Steve Granick, Active colloids with collective mobility status and research opportunities, *Chem. Soc. Rev.* **46**, 5551 (2017).
 [7] Shan Jiang, Qian Chen, Mukta Tripathy, Erik Luijten, Kenneth S. Schweizer, and Steve Granick, Janus particle synthesis and assembly, *Adv. Mater.* **22**, 1060 (2010).
 [8] Niloofar Safaie and Robert C. Ferrier, Janus nanoparticle synthesis: Overview, recent developments, and applications, *J. Appl. Phys.* **127**, 170902 (2020).
 [9] Olivier Cayre, Vesselin N. Paunov, and Orlin D. Velev, Fabrication of asymmetrically coated colloid particles by microcontact printing techniques, *J. Mater. Chem.* **13**, 2445 (2003).
 [10] Liang Hong, Angelo Cacciuto, Erik Luijten, and Steve Granick, Clusters of charged Janus spheres, *Nano Lett.* **6**, 2510 (2006).
 [11] Sebastian Berger, Alla Synytska, Leonid Ionov, Klaus-Jochen Eichhorn, and Manfred Stamm, Stimuli-responsive bicomponent polymer Janus particles by “grafting from”/“grafting to” approaches, *Macromolecules* **41**, 9669 (2008).
 [12] Marco Lattuada and T. Alan Hatton, Synthesis, properties and applications of Janus nanoparticles, *Nano Today* **6**, 286 (2011).
 [13] Yan-Li Ji, Qiang Zhao, Quan-Fu An, Ling-Ling Shao, Kueir-Rarn Lee, Zhi-Kang Xu, and Cong-Jie Gao, Novel separation membranes based on zwitterionic colloid particles: Tunable selectivity and enhanced antifouling property, *J. Mater. Chem. A* **1**, 12213 (2013).
 [14] Shuidong Huo, Ying Jiang, Akash Gupta, Ziwen Jiang, Ryan F. Landis, Singyuk Hou, Xing-Jie Liang, and Vincent M. Rotello, Fully zwitterionic nanoparticle antimicrobial agents through tuning of core size and ligand structure, *ACS Nano* **10**, 8732 (2016).
 [15] Jianxi Liu, Kaiguang Yang, Wenya Shao, Senwu Li, Qi Wu, Shen Zhang, Yanyan Qu, Lihua Zhang, and Yukui Zhang, Synthesis of zwitterionic polymer particles via combined distillation precipitation polymerization and click chemistry for highly efficient enrichment of glycopeptide, *ACS Appl. Mater. Interfaces* **8**, 22018 (2016).
 [16] Khaoula Lebdioua, Manuella Cerbelaud, Anne Aimable, and Arnaud Videcoq, Study of the aggregation behavior of Janus particles by coupling experiments and Brownian dynamics simulations, *J. Colloid Interface Sci.* **583**, 222 (2021).
 [17] Thompson Delon, Tanushree Parsai, Ufuk Kilic, Mathias Schubert, Stephen A. Morin, and Yusong Li, Impacts of

- particle surface heterogeneity on the deposition of colloids on flat surfaces, *Environ. Sci.* **8**, 3365 (2021).
- [18] John G. Kirkwood and B. Y. Shumaker, The influence of dipole moment fluctuations on the dielectric increment of proteins in solution, *Proc. Natl. Acad. Sci. U.S.A.* **38**, 855 (1952).
- [19] Mikael Lund and Bo Jönsson, On the charge regulation of proteins, *Biochemistry* **44**, 5722 (2005).
- [20] Pinaki R. Majhi, Reddy R. Ganta, Ram P. Vanam, Emek Seyrek, Katie Giger, and Paul L. Dubin, Electrostatically driven protein aggregation: β -lactoglobulin at low ionic strength, *Langmuir* **22**, 9150 (2006).
- [21] Emanuela Bianchi, Gerhard Kahl, and Christos N. Likos, Inverse patchy colloids: From microscopic description to mesoscopic coarse-graining, *Soft Matter* **7**, 8313 (2011).
- [22] Monika Stipsitz, Gerhard Kahl, and Emanuela Bianchi, Generalized inverse patchy colloid model, *J. Chem. Phys.* **143**, 114905 (2015).
- [23] Anže Lošdorfer Božič and Rudolf Podgornik, Symmetry effects in electrostatic interactions between two arbitrarily charged spherical shells in the Debye-Hückel approximation, *J. Chem. Phys.* **138**, 074902 (2013).
- [24] Yuriy V. Kalyuzhnyi, Emanuela Bianchi, Silvano Ferrari, and Gerhard Kahl, Theoretical and numerical investigations of inverse patchy colloids in the fluid phase, *J. Chem. Phys.* **142**, 114108 (2015).
- [25] Amit Goyal, Carol K. Hall, and Orlin D. Velev, Phase diagram for stimulus-responsive materials containing dipolar colloidal particles, *Phys. Rev. E* **77**, 031401 (2008).
- [26] Matthew C. Hagy and Rigoberto Hernandez, Dynamical simulation of dipolar Janus colloids: Equilibrium structure and thermodynamics, *J. Chem. Phys.* **137**, 044505 (2012).
- [27] Joshua M. Dempster and Monica Olvera de la Cruz, Aggregation of heterogeneously charged colloids, *ACS Nano* **10**, 5909 (2016).
- [28] Barry W. Ninham and V. Adrian Parsegian, Electrostatic potential between surfaces bearing ionizable groups in ionic equilibrium with physiologic saline solution, *J. Theor. Biol.* **31**, 405 (1971).
- [29] William Bailey Russel, Dudley A. Saville, and William Raymond Schowalter, *Colloidal Dispersions* (Cambridge University Press, Cambridge, England, 1991).
- [30] Gary M. C. Ong, Alejandro Gallegos, and Jianzhong Wu, Modeling surface charge regulation of colloidal particles in aqueous solutions, *Langmuir* **36**, 11918 (2020).
- [31] Tomer Markovich, David Andelman, and Rudi Podgornik, Charge regulation: A generalized boundary condition?, *Europhys. Lett.* **113**, 26004 (2016).
- [32] Arghya Majee, Markus Bier, and Rudolf Podgornik, Spontaneous symmetry breaking of charge-regulated surfaces, *Soft Matter* **14**, 985 (2018).
- [33] Kyohei Takae and Hajime Tanaka, Hydrodynamic simulations of charge-regulation effects in colloidal suspensions, *Soft Matter* **14**, 4711 (2018).
- [34] Jiaxing Yuan and Yanwei Wang, Conformation and ionization behavior of charge-regulating polyelectrolyte brushes in a poor solvent, *J. Phys. Chem. B* **125**, 10589 (2021).
- [35] Alexandre P. dos Santos and Yan Levin, Like-Charge Attraction Between Metal Nanoparticles in a 1:1 Electrolyte Solution, *Phys. Rev. Lett.* **122**, 248005 (2019).
- [36] Tine Curk and Erik Luijten, Charge Regulation Effects in Nanoparticle Self-Assembly, *Phys. Rev. Lett.* **126**, 138003 (2021).
- [37] Tine Curk, Jiaxing Yuan, and Erik Luijten, Accelerated simulation method for charge regulation effects, *J. Chem. Phys.* **156**, 044122 (2022).
- [38] J. M. Caillol, D. Levesque, and J. J. Weis, Critical Behavior of the Restricted Primitive Model, *Phys. Rev. Lett.* **77**, 4039 (1996).
- [39] M. J. Stevens and K. Kremer, Structure of Salt-Free Linear Polyelectrolytes, *Phys. Rev. Lett.* **71**, 2228 (1993).
- [40] Jacob N. Israelachvili, *Intermolecular and Surface Forces*, 3rd ed. (Academic, San Diego, 2011).
- [41] David J. Wales and Sidika Ulker, Structure and dynamics of spherical crystals characterized for the Thomson problem, *Phys. Rev. B* **74**, 212101 (2006).
- [42] R. W. Hockney and J. W. Eastwood, *Computer Simulation Using Particles* (IOP Publishing, Bristol, 1988).
- [43] See Supplemental Material at <http://link.aps.org/supplemental/10.1103/PhysRevLett.128.158001> for information about the additional model details and parameters, the simulation method of charge regulation, the anisotropic charge regulation, the dependence of the ionization degree on $\Delta pH = pH - pK$, the effect of reservoir salt concentration, the effect of electrostatic coupling strength, and the limitations of the model, which includes Refs. [44–47].
- [44] Jonas Landsgesell, Pascal Hebbeker, Oleg Rud, Raju Lunkad, Peter Košovan, and Christian Holm, Grand-reaction method for simulations of ionization equilibria coupled to ion partitioning, *Macromolecules* **53**, 3007 (2020).
- [45] Kipton Barros and Erik Luijten, Dielectric Effects in the Self-Assembly of Binary Colloidal Aggregates, *Phys. Rev. Lett.* **113**, 017801 (2014).
- [46] Akira Furukawa and Hajime Tanaka, Key Role of Hydrodynamic Interactions in Colloidal Gelation, *Phys. Rev. Lett.* **104**, 245702 (2010).
- [47] Michio Tateno and Hajime Tanaka, Numerical prediction of colloidal phase separation by direct computation of Navier-Stokes equation, *npj Comput. Mater.* **5**, 40 (2019).
- [48] Alessandro Barducci, Giovanni Bussi, and Michele Parrinello, Well-Tempered Metadynamics: A Smoothly Converging and Tunable Free-Energy Method, *Phys. Rev. Lett.* **100**, 020603 (2008).
- [49] Giacomo Fiorin, Michael L. Klein, and Jérôme Hémin, Using collective variables to drive molecular dynamics simulations, *Mol. Phys.* **111**, 3345 (2013).
- [50] Mikael Lund and Bo Jönsson, Charge regulation in biomolecular solution, *Q. Rev. Biophys.* **46**, 265 (2013).
- [51] Anna Stradner, Helen Sedgwick, Frédéric Cardinaux, Wilson C. K. Poon, Stefan U. Egelhaaf, and Peter Schurtenberger, Equilibrium cluster formation in concentrated protein solutions and colloids, *Nature (London)* **432**, 492 (2004).
- [52] M. Cerbelaud, R. Ferrando, and A. Videcoq, Simulations of heteroaggregation in a suspension of alumina and silica

particles: Effect of dilution, *J. Chem. Phys.* **132**, 084701 (2010).

[53] Zhi Yong Ju and Arun Kilara, Gelation of *pH*-aggregated whey protein isolate solution induced by heat, protease,

calcium salt, and acidulant, *J. Agric. Food Chem.* **46**, 1830 (1998).

[54] Jan Antosiewicz, Computation of the dipole moments of proteins, *Biophys. J.* **69**, 1344 (1995).